Supplementary material

Text S1. The detailed information of Moran's I

global Moran's *I* (I) can be expressed as:

$$I=\left[\frac{N}{\sum_{i=1}^{N}\sum_{j=1}^{N}w_{ij}}\right]\left[\frac{\sum_{i=1}^{N}\sum_{J=1}^{N}\Omega_{ij}(Z_i-\overline{Z})(Z_j-\overline{Z})}{\sum_{i=1}^{N}(Z_i-\overline{Z})^2}\right] \quad \text{equation (1)}$$

where N is the number of points, with i and j taking values from 1 to N, assuming that there are n spatial samples. $\overline{Z}$ is the mean value of Z; Z_i and Z_j are the values of variable atlocations i and j, respectively ($i \neq j$); and w_{ij} is the spatial weight describing the adjacency of distance between the i^{th} and j^{th} point[1,2]. A single value is used to reflect the degree of autocorrelation of variables. When calculating the global Moran's *I* statistics, two parameters, Z(I) and *P*-value provide the calculated Moran's I statistics statistical significance[3]. The Z(I) is calculated as follows:

$$Z(I)=(I-E(I)/\sqrt{Var(I)}) \quad \text{equation (2)}$$

where I represents Moran's I, and E(I) and Var(I) are the theoretical expectation and variance of Moran's I, respectively.

While global Moran's *I* represent the presence or absence of spatial autocorrelation as a whole, Anselin (1995)[3] defines such local correlation statistics as local indicators of spatial correlation (LISA), which can be used to detect spatial clustering or "hot spots". The local Moran's *I* is one of LISA, represents the significant spatial clustering of similar values around a particular observation[4,5]. The statistic for Local Moran's *I* is defined as:

$$I_i=\frac{Z_i-\overline{Z}}{\sigma^2}\sum_{j=1 j\neq i}^{N}\left[w_{ij}(Z_j-\overline{Z})\right] \quad \text{equation (3)}$$

Where $\overline{Z}$ is the mean value of Z with the sample number of n; Z_i is the value of the variable at location i; Z_j is the value at other locations (where $j \neq i$); σ^2 is the variance of Z; and W_{ij} is a distance weighting between Z_i and Z_j.

Local Moran's *I* can detect spatial outliers, locates spatial associations, and identifies local clusters[1,5]. The local Moran's *I* index was applied to identify the soil properties cluster in this study. Global Moran's I and local Moran's *I* were calculated using the GeoDa software (Version 1.14).

Text S2. The detailed information of Semi-variance

The standard equation for the semivariance is given as [Eq. (4)]:

$$\gamma(h)=\frac{1}{2N(h)}\sum_{i=1}^{N(h)}\left[Z(x_j)-Z(x_i+h)\right]^2 \quad \text{equation (4)}$$

where γ (h) is the experimental semivariance value at distance interval h (km) and describes the degree of autocorrelation, $Z(x_i)$ and $Z(x_i+h)$ are the measured sample value at grid x_i and sample value at x_i+h, respectively, and N(h) is the total number of sample data pairs within distance h (km). The following parameters are applied to identify the semivariance functions[6-9]: sill (C_0+C), range (A_0), nugget effect (C_0), spatially dependent structural variance (C), and the ratio of the Nugget effect (C_0) to the Sill (C_0+C). The "Nugget to-sill" ratio ([$C_0/(C_0+C)$]) is an important indicator to measure the extent of spatial dependence of variables in soil[10]. The ratio < 0.25 indicates that the studied variable has a strong spatial dependencies, which is mainly controlled by intrinsic variation, such as topography, soil type, parent material, climate. The ratio between 0.25 and 0.75 shows moderate spatial dependence of the studied variable. The ratio > 0.75 reveals that the study variable has weak spatial dependence, and is mainly affected by external factors (human activities, such as mining, road traffic, fertilization, tillage, planting system, land use intensity, etc.). The experimental semivariance was fitted by exponential model, Gaussian model, spherical model and linear model. Analysis of semivariance was carried out with GS+ (Version 7.0).

Figure S1. Comparison of knock and net harvesting. a and b represent knock harvesting, c and d represent net harvesting.

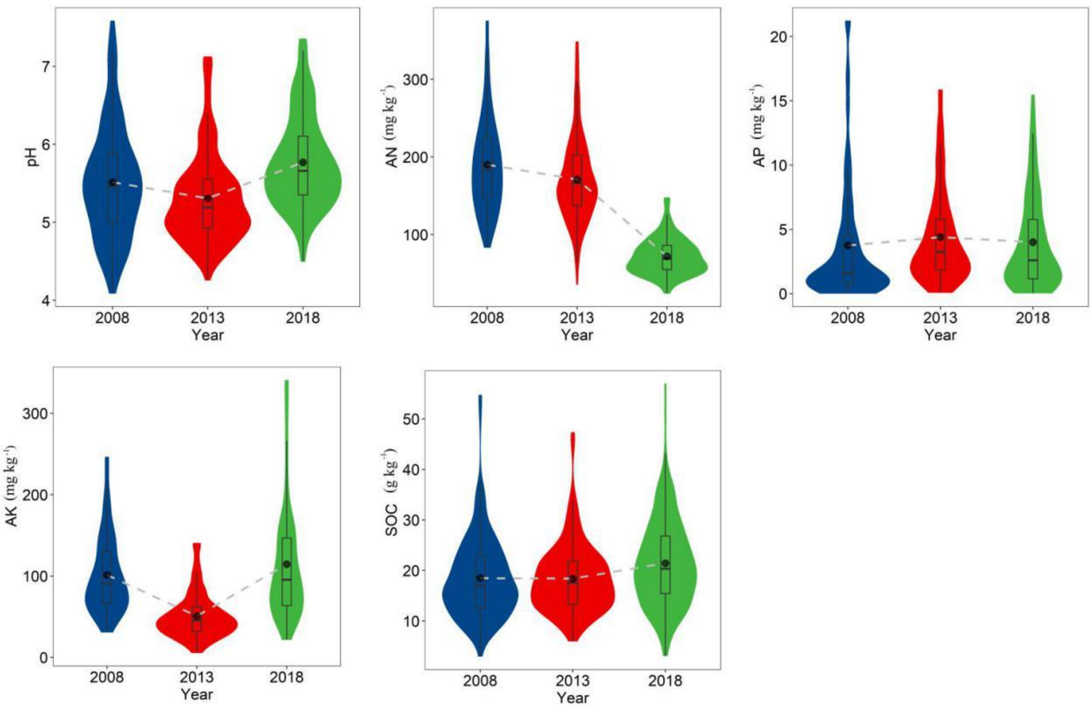

Figure S2. Kernel density estimation of soil properties in 2008, 2013 and 2018. Black points represent the mean value and black box represent the distributions of quarter value, median value and three-quarters value. AN: available nitrogen; AP: available phosphorus; AK: available potassium; SOC: soil organic carbon.

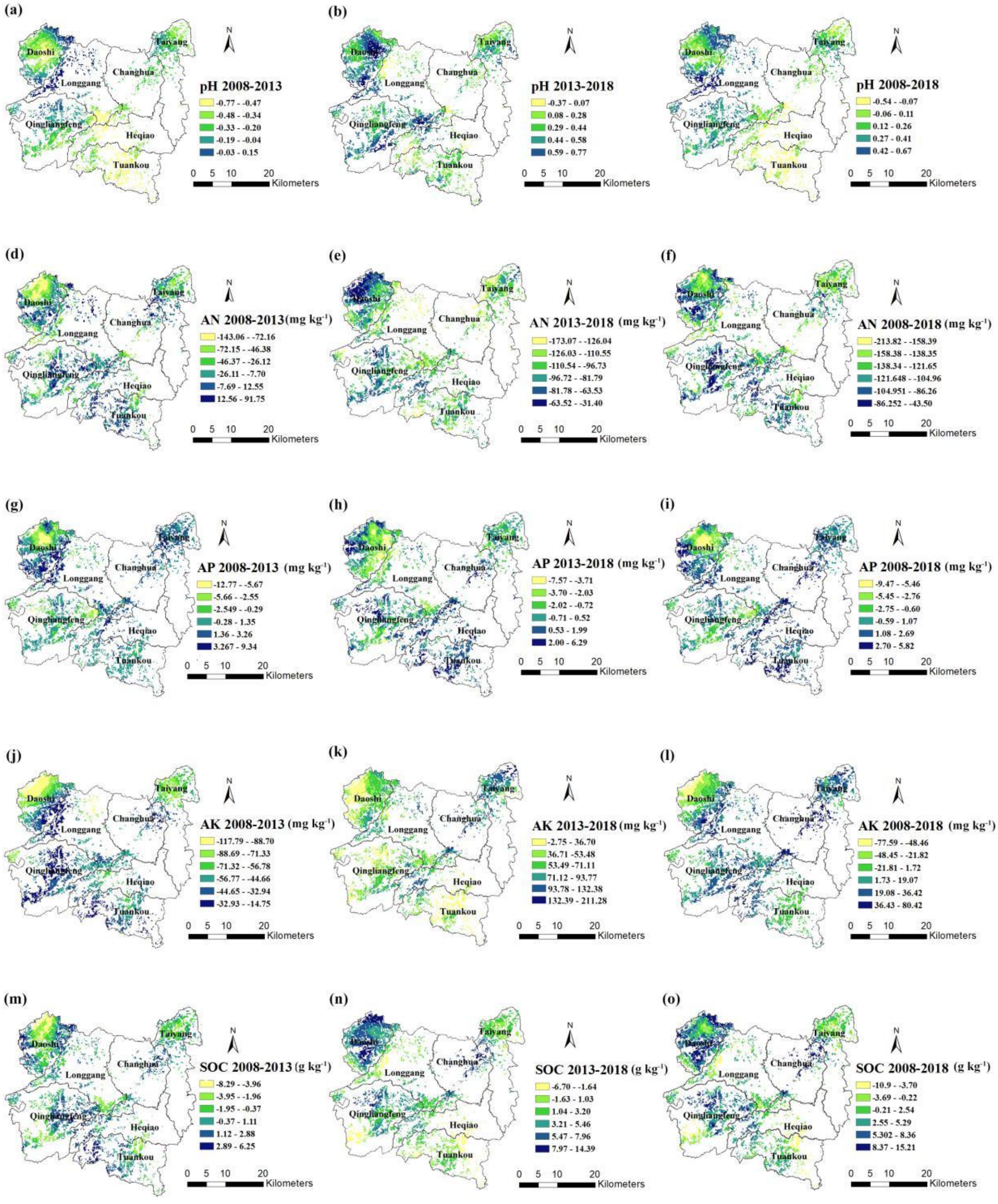

Figure S3. Spatial variation of the change of soil properties in hickory plantation regions. AN: available nitrogen; AP: available phosphorus; AK: available potassium; SOC: soil organic carbon.

Figure S4. Overuse of herbicides causes death of hickory

Table S1. Thresholds values for soil properties indices.

	pH	AN (mg kg^{-1})	AP (mg kg^{-1})	AK (mg kg^{-1})	SOC (g kg^{-1})
x_a	4.5	60	5	50	5.8
x_b	5.5	120	10	100	11.6
x_c	6.5	180	20	200	17.4

x_a, x_b and x_c are the upper and lower limits of each classification standard, respectively. AN: available nitrogen; AP: available phosphorus; AK: available potassium; SOC: soil organic carbon.

Table S2. Main effect factors of the change in soil properties.

Attributes	Factors	Type IIIsum of squares	df	Mean square	The F statistic	F value with probability
C_{pH}	Altitude	2.552	3	0.851	2.504	0.06
	Mean annual precipitation	7.684	2	3.842	7.667	0.001***
	Mean annual temperature	13.507	3	4.502	9.935	0.001***
	Parent material	2.607	6	0.434	1.271	0.272
	Forest age	1.576	3	0.525	1.005	0.393
	Fertilizer	3.482	2	1.741	5.261	0.006**
	Harvest method	5.621	4	1.405	4.343	0.002**
	Weeding method	4.813	2	2.406	7.419	0.001***
C_{AN}（mg kg^{-1}）	Altitude	9150.211	3	3050.070	5.922	0.001***
	Mean annual precipitation	14417.277	2	7208.639	1.983	0.142
	Mean annual temperature	31026.333	3	10342.111	2.94	0.036*
	Parent material	4548.592	6	758.099	1.402	0.216
	Forest age	18798.416	3	6266.139	1.776	0.154
	Fertilizer	7313.444	4	1828.361	3.504	0.009**
	Harvest method	6121.085	1	6121.085	11.771	0.001***
	Weeding method	3301.337	2	1650.668	3.077	0.048*
C_{AP}（mg kg^{-1}）	Altitude	154.680	3	51.560	4.003	0.009**
	Mean annual precipitation	87.538	2	43.769	1.431	0.244
	Mean annual temperature	251.901	3	83.967	2.857	0.04*
	Parent material	149.741	6	24.957	1.922	0.079
	Forest age	78.551	3	26.184	0.905	0.441
	Fertilizer	158.985	4	39.746	3.103	0.017*
	Harvest method	131.917	1	131.917	10.344	0.002**
	Weeding method	192.347	2	96.174	7.682	0.001***
C_{AK}（mg kg^{-1}）	Altitude	29083.165	3	9694.388	2.012	0.114
	Mean annual precipitation	19263.247	2	9631.623	1.484	0.231
	Mean annual temperature	34908.457	3	11636.152	1.816	0.148
	Parent material	29276.957	6	4879.493	1.006	0.423
	Forest age	14823.104	3	4941.035	0.709	0.548
	Fertilizer	50958.698	4	12739.675	2.713	0.031*
	Harvest method	14803.068	1	14803.068	3.082	0.081
	Weeding method	18606.03	2	9303.015	1.935	0.147
C_{SOC}（g kg^{-1}）	Altitude	1091.888	3	363.963	5.650	0.001***
	Mean annual precipitation	237.919	2	118.959	1.329	0.269
	Mean annual temperature	347.224	3	115.741	1.296	0.28
	Parent material	467.790	6	77.965	1.138	0.342
	Forest age	188.251	3	62.750	0.631	0.596
	Fertilizer	1332.535	4	333.134	5.241	0.001***
	Harvest method	517.803	1	517.803	7.774	0.006**
	Weeding method	985.365	2	492.682	7.622	0.001***

* P<0.05, ** P<0.01, *** P<0.001. C_{pH}: change in pH; C_{AN}: change in available nitrogen; C_{AP}: change in available

phosphorus; C_{AK}: change in available potassium; and C_{SOC}: change in soil organic carbon.

Reference

1 Fu, W., Zhao, K., Zhang, C., Wu, J. & Tunney, H. Outlier identification of soil phosphorus and its implication for spatial structure modeling. *Precis. Agric.* **17**, 121-135, doi:10.1007/s11119-015-9411-z (2016).

2 Shi, A., Shao, Y., Zhao, K. & Fu, W. Long-term effect of E-waste dismantling activities on the heavy metals pollution in paddy soils of southeastern China. *Sc. Total Environ.* **705**, doi:10.1016/j.scitotenv.2019.135971 (2020).

3 Anselin, L. Local Indicators of Spatial Association—LISA. *Geogr. Anal.* **27**, 93-115, doi:10.1111/j.1538-4632.1995.tb00338.x (1995).

4 Zhao, K. *et al.* Spatial variations of concentrations of copper and its speciation in the soil-rice system in Wenling of southeastern China. *Environ. Sci. Pollut. R.* **21**, 7165-7176, doi:10.1007/s11356-014-2638-9 (2014).

5 Fu, W. *et al.* Spatial variation of biomass carbon density in a subtropical region of Southeastern China. *Forests* **6**, 1966-1981, doi:10.3390/f6061966 (2015).

6 Treitz, P. & Howarth, P. High spatial resolution remote sensing data for forest ecosystem classification: An examination of spatial scale. *Remote Sens. Environ.* **72**, 268-289, doi:10.1016/S0034-4257(99)00098-X (2000).

7 Zawadzki, J., Cieszewski, C. J., Zasada, M. & Lowe, R. C. in *Silva Fennica Monographs* Vol. 39 599-617 (2005).

8 Fu, W. J., Jiang, P. K., Zhou, G. M. & Zhao, K. L. Using Moran's i and GIS to study the spatial pattern of forest litter carbon density in a subtropical region of southeastern China. *Biogeosciences* **11**, 2401-2409, doi:10.5194/bg-11-2401-2014 (2014).

9 Chen, S., Lin, B., Li, Y. & Zhou, S. Spatial and temporal changes of soil properties and soil fertility evaluation in a large grain-production area of subtropical plain, China. *Geoderma* **357**, doi:10.1016/j.geoderma.2019.113937 (2020).

10 Cambardella, C. A. *et al.* Field-scale variability of soil properties in central Iowa soils. *Soil Sci. Soc. Am. J.* **58**, 1501-1511, doi:10.2136/sssaj1994.03615995005800050033x (1994).